Int. J. Heat Mass Transfer. Vol. 6, pp. 1063–1075. Pergamon Press 1963. Printed in Great Britain.

HEAT TRANSFER IN DISSOCIATED AIR WITH VARIABLE HEAT OF DISSOCIATION

S. J. FENSTER and R. J. HEYMAN

Denver Division, Martin-Marietta Corporation, Denver 1, Colorado, U.S.A.

(*Received* 31 *August* 1962 *and in revised form* 19 *January* 1963)

Abstract—The heat transfer through a laminar dissociated boundary layer is examined using a definition for a variable heat of dissociation that permits a distinction between oxygen and nitrogen. The results indicate that the heat transfer through an equilibrium boundary layer is somewhat less than previously reported by other investigators. Furthermore, it is found for the range of free stream conditions considered that oxygen recombination (rather than nitrogen) is the more dominant process for determining heat transfer through an equilibrium boundary layer.

NOMENCLATURE

C, $\bar{c}_p/\bar{c}_{pw}$;
c_i, mass fraction of specie i;
c_{pi}, specific heat per unit mass at constant pressure of specie i, Btu/lb degR;
$\bar{c}_p$, weighted sum of specie specific heats, Btu/lb degR;
f, defined by equation (12) as a dimensionless velocity variable;
h, enthalpy per unit mass of mixture, Btu/lb;
h_i, perfect gas enthalpy per unit mass of specie i, $c_{pi}\,T + u^2/2$, Btu/lb;
h_i^o, heat evolved in the formation of specie i at 0°K per unit mass, Btu/lb;
j, superscript, equals -1 for axisymmetric body; and $+1$ for planar body;
k, thermal conductivity, Btu/s degR ft;
L, Lewis number for atom–molecule mixture;
N, defined by equation (12);
Nu, Nusselt number;
Pr, Prandtl number, $\mu\bar{c}_p/k = 0{\cdot}71$;
q, heat flux, Btu/ft² s, kW/cm²;
r, cylindrical radius of body, ft;
Re, Reynolds number;
R, universal gas constant;
s, superscript, equals 1 for axisymmetric body and 0 for planar body;
T, absolute temperature, °R;
u, x component of velocity v, ft/s;
w_i, mass rate of formation of specie i per unit volume and time;
x, distance along surface from leading edge, ft;
y, distance normal to surface, ft;
z, defined by equation (12), dimensionless mass fraction.

Greek symbols

β, $\dfrac{2d\ln u_e}{d\ln \xi}$, equals 0 for flat plate, and 1/2 for stagnation point;
η, defined by equation (11);
θ, defined by equation (12), dimensionless temperature;
λ, defined as u_e/x for flat plate, and $(du_e/dx)_s$ for stagnation point, s^{-1};
μ, absolute viscosity, slugs/ft s;
ξ, defined by equation (10);
ρ, mass density, slugs/ft³.

Subscripts

a, atom;
e, edge of boundary layer;
E, equilibrium;
i, ith specie of mixture;
m, molecule;
n, nitrogen;
o, oxygen;

s, stagnation conditions;
w, wall;
∞, free stream.

1. INTRODUCTION

THE first complete numerical solution of the appropriate conservation equations which considered the actual dissociated state of equilibrium air was that of Moore [1]. Hansen [2] pointed out that Moore had miscalculated the Prandtl number for dissociated air, and Romig and Dore [3] carried out a similar analysis with a corrected Prandtl number variation. However, the authors employed equilibrium air properties based on an old, incorrect value of the dissociation energy of nitrogen. Both the above solutions are valid only under the restriction that the Lewis number is exactly 1, and there is no way in which the results can be extrapolated to the case where $L \neq 1$. This follows from the fact that with $L \neq 1$ the heat transfer is no longer simply proportional to the enthalpy difference across the boundary layer, but also involves the extent to which the energy of dissociation contained in the flow is transferred.

Stagnation point heat transfer in a dissociated gas has been treated rather extensively by Fay and Riddell [4], who included constant Lewis numbers from 1 to 2, variable specific heat, variable $\rho\mu$, constant Prandtl number, and equilibrium and nonequilibrium flows; and by Scala and Baulknight [5], who treated the problem in a manner similar to Fay and Riddell, but also included variable Lewis and Prandtl numbers plus thermal diffusion. Based upon gross heat transfer to a stagnation point surface for given environmental conditions, agreement between [4] and [5] is within 10 per cent for moderate altitudes. The boundary layer characteristics for a dissociated flow over a flat plate with $L \neq 1$ have not been treated although Wilson [6] has obtained gross skin friction and heating rates by an integral method where diffusion effects were neglected.

It is believed that the most comprehensive treatment of the dissociated air problem has been that of [4] and [5], in which the gas is considered to be a binary mixture of air atoms and air molecules. The primary constituents of air, oxygen and nitrogen are quite similar insofar as transport properties (i.e. viscosity, thermal conductivity, and diffusion) are concerned. Their principle difference lies in the molecular binding energies which are in the ratio of nearly 2 to 1 (nitrogen: 9·76 eV and oxygen: 5·1 eV). Therefore, air may reasonably be considered a binary mixture insofar as transport properties are concerned but not in regard to chemical reaction, since equal amounts of heat will not be released for every atom pair recombination in contrast to the assumption of equal heat release in [4] and [5]. Consequently, it is the purpose of this paper to use a variable heat of dissociation that allows for the distinction between oxygen and nitrogen, in order to obtain solutions for the laminar boundary layer at a stagnation point and on a flat plate in dissociated air.

2. EQUATIONS OF MOTION

The equations of motion for the real gas laminar boundary layer have been developed in some detail in [4] and are given as*

$$(\rho r u)_x + (\rho r v)_y = 0 \tag{1}$$

$$\rho u c_{ix} + \rho v c_{iy} = (\rho D_i c_{iy})_y + w_i \tag{2}$$

$$\rho \mathbf{v} \cdot \operatorname{grad} h = (kT_y)_y + uP_x + \mu(u_y)^2 + \left[\sum_i D_i \rho c_{iy}(h_i - h_i^o)\right]_y \tag{3}$$

where thermal diffusion has been neglected. If as in [4],

$$h = \sum c_i(h_i - h_i^o)$$

$$\operatorname{grad} h = \sum c_i(\mathrm{d}h_i/\mathrm{d}T) \operatorname{grad} T + \sum (h_i - h_i^o) \operatorname{grad} c_i$$

and

$$\bar{c}_p \equiv \sum c_i (\mathrm{d}h_i/\mathrm{d}T) = \sum c_i c_{pi}$$

then the energy equation in combination with (2) can be written in terms of the dependent variable T as

$$\bar{c}_p(\rho u T_x + \rho v T_y) = (kT_y)_y + uP_x + \mu(u_y)^2 + \sum w_i (h_i^o - h_i) - \sum (h_i - h_i^o)(\rho D_i c_{iy})_y + [\sum (h_i - h_i^o) \rho D_i c_{iy}]_y. \tag{4}$$

Considering h_a^o as constant results in the energy equation of [4], namely,

$$\bar{c}_p (\rho u T_x + \rho v T_y) = (kT_y)_y + uP_x + \mu(u_y)^2 + \sum w_i (h_i^o - h_i) + \sum c_{pi} D_i \rho c_{iy} T_y \tag{5}$$

* Where D_i = diffusion coefficient, subscripts x and y denote partial derivatives, and P is the absolute pressure.

for a gas at equilibrium. However, when h_a^o is considered to be a variable the energy equation (4) becomes

$$\bar{c}_p(\rho u T_x + \rho v T_y) = (kT_y)_y + uP_x + \mu(u_y)^2 + \sum w_i(h_i^o - h_i) + \sum \rho D_i c_{iy}(c_{pi} T_y - h_{iy}^o). \quad (6)$$

If the local similarity concept is now employed as in [4] the equations of motion (1), (2) and (6) become in dimensionless form

$$(Nf_{\eta\eta})_\eta + ff_{\eta\eta} + \beta\left(\frac{\rho_e}{\rho} - f_n^2\right) = 0 \quad (7)$$

$$\left(\frac{NL\, z_{i\eta}}{Pr}\right)_\eta + \frac{2^j \lambda^{-1} w_i}{\rho c_{ie}} + f z_{i\eta} = 0 \quad (8)$$

$$\left(\frac{CN\theta_\eta}{Pr}\right)_\eta + Cf\theta_\eta + \sum_i \frac{2^j \lambda^{-1} w_i (h_i^o - h_i)}{\rho \bar{c}_{pw} T_e} + \frac{Nu_e^2}{\bar{c}_{pw} T_e} f_{\eta\eta}^2 + \sum_i \frac{NL\, c_{i\eta}}{Pr \bar{c}_{pw}} (c_{pi}\theta_\eta - h_{i\eta}^o/T_e) = 0. \quad (9)$$

Where the binary mixture assumption has been used to take advantage of the use of a single diffusion coefficient, and subscript η refers to differentiation with respect to η. Further,

$$\xi(x) = \int_0^x \rho_w \mu_w u_e r^{2s}\, dx,\ d\xi/dx = \rho_w \mu_w u_e r^{2s}; \quad (10)$$

and

$$\eta(x, y) = [u_e r^s (2\xi)^{\frac{1}{2}}] \int_0^y \rho\, dy,\ \partial\eta/\partial y = r^s \rho u_e (2\xi)^{1/2}. \quad (11)$$

The dimensionless dependent variables are defined as follows:

$$\left.\begin{aligned} f &= \int_0^\eta f_\eta\, d\eta, f_\eta = u/u_e \\ \theta &= T/T_e \\ z &= c_i/c_{ie} \\ N &= \rho\mu/\rho_w \mu_w, \end{aligned}\right\} \quad (12)$$

with

$$j = -1,\ s = 1,\ \lambda = (du_e/dx)_s,\ \beta = 1/2$$

defining the stagnation point problem and

$$j = 1,\ s = 0,\ \lambda = u_e/x,\ \beta = 0,$$

the flat plate. Also, it is to be noted that in the case of the stagnation point, the term $(Nu_e^2/\bar{c}_{pw} T_e) f_{\eta\eta}^2$ is small for high velocity flows and can be neglected.

3. METHOD OF ANALYTICAL SOLUTION

A. Equilibrium boundary layer

Complete thermodynamic equilibrium requires that the gas properties and concentrations of atoms and molecules be identical with their equilibrium values appropriate to the local temperature at every point of the flow. Here the chemical reaction rates are considered very fast relative to the rates of convection along streamlines or diffusion across streamlines. That is to say that the recombination rate is sufficiently large to maintain thermodynamic equilibrium. Hence, the solution of the equilibrium boundary layer is obtained by eliminating the term $2^j \lambda^{-1} w_i/\rho$ between equations (8) and (9) and solving the resulting equation

$$\left(\frac{CN\theta_\eta}{Pr}\right)_\eta + Cf\theta_\eta + \sum_i \frac{c_{ie}(h_i - h_i^o)}{\bar{c}_{pw} T_e}\left[\left(\frac{NL z_{i\eta}}{Pr}\right)_\eta + f z_{i\eta}\right] + \frac{Nu_e^2}{\bar{c}_{pw} T_e} f_{\eta\eta}^2 + \frac{NL}{Pr\, \bar{c}_{pw}} \sum_i c_{i\eta}(c_{pi}\theta_\eta - h_{i\eta}^o/T_e) = 0 \quad (13)$$

simultaneously with (7).

The equilibrium atom mass fractions are taken from the tables of Logan and Traenor [7] and are approximated at constant pressure by an exponential of the form $C_{aE} = C_{ae}\, e^{\alpha(1-1/\theta)}$ where α is a constant. The Prandtl number was assumed constant at 0·71, the Lewis number was taken as a function of temperature and density as determined by Hansen [8], and the viscosity temperature relation was that of Penner and Litvak as reported by Fay and Riddell [4]. In addition, the ratios ρ_e/ρ and $\bar{c}_p/\bar{c}_{pw}$ were determined as in [4].

As previously mentioned, the binary mixture assumption may not be valid insofar as chemical reaction is concerned, since, nitrogen and oxygen atoms will recombine to their equilibrium concentrations appropriate to their equilibrium temperatures with a release in energy of 9·76 eV

for n and 5·1 eV for o. Furthermore, as the atoms diffuse towards the wall they first diffuse into regions sufficiently cool to initiate nitrogen recombination. From equilibrium mass fraction tables it is observed that practically all the nitrogen atoms will recombine before oxygen recombination commences in the very cool regions near the wall. This then allows the use of atom mass fraction "c_a" directly for the dissociation energy term

$$h_a^o = -h_o^o, \; c_a < 0{\cdot}2346$$

$$h_a^o = \frac{0{\cdot}2346(-h_o^o) + (c_a - 0{\cdot}2346)(-h_n^o)}{c_a}, \quad c_a \geq 0{\cdot}2346. \qquad (14)$$

This equation was used by Goulard [9] but only at the equilibrium edge of a frozen boundary layer. However, its use here is applied throughout the entire boundary layer. Furthermore, equation (14) shows that below $C_a = 0{\cdot}2346$ only oxygen atoms will exist. This is not rigorously correct but will be shown to be a valid approximation in a succeeding section. In addition, it was also assumed that the term $N c_{i\eta} h_{i\eta}^o / T_e$ in the energy equation would have a negligible contribution since $h_{i\eta}^o$ is zero until $c_a = 0{\cdot}2346$ while $c_{i\eta} \to 0$ quite rapidly near the edge of the boundary layer. Also, N decreases with increasing η.

In order to compare the effect of the variable heat of dissociation to previous solutions, the method of Fay–Riddell [4] with a variable Lewis number and a constant heat of dissociation

$$h_{ae}^o = \frac{\sum_{\text{atoms}} c_{ie}(-h_i^o)}{\sum_{\text{atoms}} c_{ie}} \qquad (15)$$

was obtained and hereafter noted as Method 1. The solution obtained with both a variable Lewis number and variable heat of dissociation is then termed Method 2 (see Appendix A for the method of machine solution).

B. Frozen boundary layer

In the case of frozen flow, chemical reaction rates are very slow compared to the diffusion rate across stream lines so that no net mass rate of formation occurs ($w_i = 0$). Furthermore, since there is no net mass rate of formation, h_a^o will be constant at the value h_{ie}^o so that $h_{i\eta}^o$ is zero. In addition, the atom concentration is no longer a unique function of the temperature and pressure so that an additional *continuity of species* equation must be included. Hence, equations (7–9) must be solved simultaneously.

C. Boundary conditions

The boundary conditions to be used with equations (7–9) are dependent on the state of the external flow and the wall temperature and catalytic efficiency. The flow cases considered here are the limits of equilibrium and fully frozen flows, Mach numbers from 10 to 24, with wall temperatures from 300 to 1000°K, and wall catalytic efficiencies from 0 to 100 per cent. Thus, the boundary conditions are

$$f(0) = f_\eta(0) = 0, \qquad \theta(0) = \theta_w = T_w/T_e,$$
$$f_\eta(\infty) = 1, \qquad \theta(\infty) = 1,$$
$$z(0) = 0,\ 0{\cdot}5,\ 1{\cdot}0,$$
$$z(\infty) = 1.$$

4. HEAT TRANSFER

Ignoring radiation and ionization, heat is transferred to a surface by molecular conduction and atomic diffusion, the latter being included only when the atoms recombine at the wall. The heat-transfer rate describing both such modes in terms of the transformed co-ordinates is

$$q_w = (0{\cdot}707)^j (\rho_w \mu_w)^{1/2} Pr^{-1} \bar{c}_{pw} T_e \theta_\eta(0) \left[1 + \frac{c_{ae} h_a^o L_w}{\bar{c}_{pw} T_e} \frac{z_\eta(0)}{\theta_\eta(0)}\right] \qquad (16)$$

where h_a^o is evaluated at the wall for equilibrium flow and at the edge of the boundary layer for frozen flow.

It is also possible to define Nusselt and Reynolds numbers based on the local co-ordinate x. Thus, defining

$$Nu_w = q_w x \bar{c}_{pw} / k_w (h_e - h_w)$$

and

$$Re_w = \rho_w u_e x / \mu_w,$$

the heat-transfer parameter at the wall may be written as

$$[Nu/(Re)^{1/2}]_w = (0{\cdot}707)^j \frac{\bar{c}_{pw} T_e \theta_\eta(0)}{h_e - h_w} \left[1 + \frac{c_{ae} L_w h_a^o z_\eta(0)}{\bar{c}_{pw} T_e \theta_\eta(0)}\right]. \quad (17)$$

The parameters $z_\eta(0)$ and $\theta_\eta(0)$ must now be determined by solution of the boundary-layer equations as discussed in the previous section. The following sections discuss such solutions under the various boundary and flow conditions considered here.

5. RESULTS AND DISCUSSION

Solution of the equations of motion (7–9) for the stagnation point and flat plate were obtained using both the definitions of heat of dissociation of Method 1 and 2. As would be expected, the equilibrium heat-transfer rates of Method 2 are significantly lower than those of Method 1 when the degree of free stream dissociation is large; however, for small amounts of free stream dissociation, the two methods tend to yield the same result.

A. Stagnation point characteristics

The machine solution of equations (7–9) with $\beta = 1/2$ yield the distribution of θ, f_η, and z through the laminar boundary layer as a function of η. Typical profiles of θ and c_a with recombination energies determined by both Methods 1 and 2, are shown in Figs. 1 and 2 for equilibrium and frozen flows at a stagnation point. Tables containing pertinent parameters are shown in Appendix B.

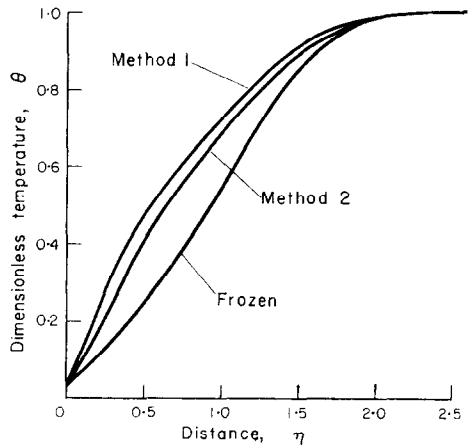

FIG. 1. Temperature distribution through a laminar boundary layer at a stagnation point, altitude = 75 000 ft.

Referring to Fig. 2 it may be seen that the equilibrium atom mass fraction obtained by Method 1 is equal to the frozen atom mass fraction at $\eta = 1{\cdot}1$ let us select this point to examine the equilibrium composition. The machine solution reveals that at this value of η, $\theta = 0{\cdot}7635$. Equilibrium tables [7] show that along a line of constant pressure appropriate to the stipulated flight conditions of Fig. 2, the

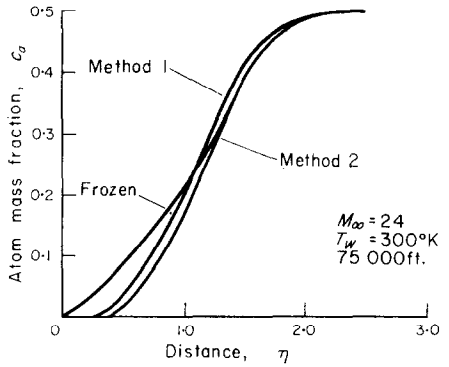

FIG. 2. Atom mass fraction distribution through a laminar boundary layer at a stagnation point, altitude = 75 000 ft.

mole fraction of nitrogen atoms is almost an order of magnitude lower than the mole fraction of oxygen atoms. However, the Method 1 definition h_a^o calls for a recombination energy at this point equivalent to that at the edge of the boundary layer, but at the edge of the equilibrium boundary layer the mole fraction of nitrogen atom is actually greater than that of the oxygen atom. The Method 1 definition of h_a^o then yields a value which is dominated by the nitrogen bond energy at $\eta = 1{\cdot}1$ while for all practical purposes only oxygen atoms exist from this point to the wall and only the heat of formation of oxygen should be released.

This paradox does not occur with the Method 2 solution. At $\eta = 1{\cdot}2$, $c_a = 0{\cdot}2346$, according to equation (11) all the nitrogen atoms will have recombined and only oxygen atoms will be left to recombine below this point. In reality, the nitrogen cutoff point of $c_a^* = 0{\cdot}2346$ is not

as abrupt as equation (11) implies. Actually, some nitrogen atoms exist below this point and will be available for recombination. However, there are so few that their contribution is not felt. This has been shown by setting the nitrogen cutoff point down to $c_a^* = 0{\cdot}15$ and observing no significant changes (see Table 2).

In addition several cases were computed inserting the term $Nc_{i_\eta} h_{i_\eta}^o/T_e$ [see equation (13)]. In the most severe case considered, $M_\infty = 24$, altitude = 75 000 ft, the correction amounted to about a 7 per cent increase in the total heat transfer rate and thus the approximation is justified.

A further illustration of this difference has been pointed out in [10] and may be seen in Figs. 3 and 4, where the distribution of heat of

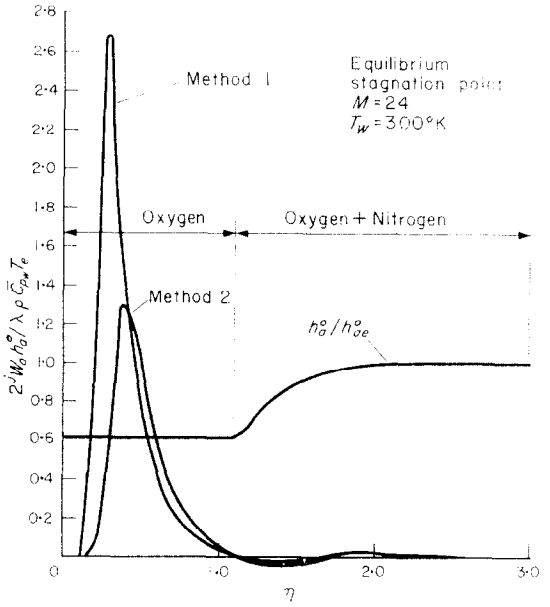

FIG. 3. Normalized chemical reaction energy and heat of dissociation distributions through a laminar boundary layer at a stagnation point, altitude = 75 000 ft.

formation and the normalized energy due to chemical reactions is plotted for the cases $M_\infty = 24$, $T_w = 300°K$, at 75 000 and 250 000 ft altitudes.

Furthermore, Figs. 3 and 4 reveal that the chemical energy available for heating is primarily oxygen-controlled, as seen by the fact that the

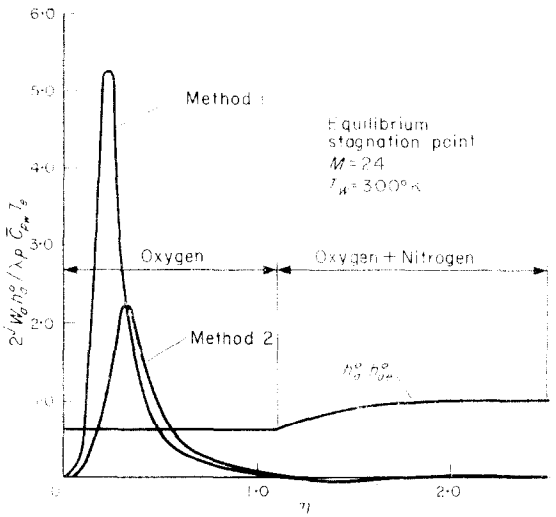

FIG. 4. Normalized chemical reaction energy and heat of dissociation distributions through a laminar boundary layer at a stagnation point, altitude = 250 000 ft.

chemical reaction energy term is essentially zero at the point where the dissociation energy of nitrogen becomes available and thereafter remains small. This effect was observed for all cases considered and is a rather surprising result, since the nitrogen atom mass fraction for some cases is greater than that of oxygen. However, the nitrogen atoms recombine in the outer regions of the boundary layer so that their contribution to the chemical reaction energy term is small.

At a much lower Mach number, $M_\infty = 10$, for the same environmental conditions, the chemical reaction energies for the two methods coincide, as might be expected, since the definitions of h_a^o of Methods 1 and 2 become identical (see Fig. 5).

The values of $\theta_\eta(0)$ and $z_\eta(0)$ obtained from the solution of the equations of motion when substituted into equation (17) yield values of $Nu/(Re)^{1/2}$ for each Mach number, wall temperature, and altitude considered. These results are plotted in Fig. 6 for both equilibrium and frozen flow with $z(0) = 0$. Also shown in Fig. 6 is a correlation curve obtained by a least-squares fit of the points shown. These equations are given for equilibrium and frozen flow respectively, with $z(0) = 0$, by

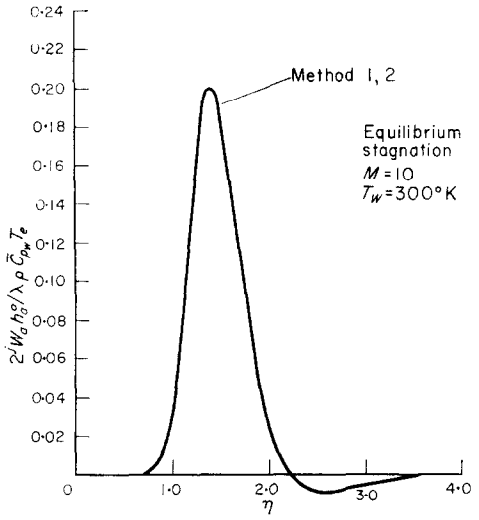

FIG. 5. Normalized chemical reaction energy distribution through a laminar boundary layer at a stagnation point, altitude = 75 000 ft.

$$[Nu/(Re)^{1/2}]_w = 0{\cdot}753\ N_e^{0{\cdot}595}; \qquad (18)$$

$$[Nu/(Re)^{1/2}]_w = 0{\cdot}603\ N_e^{0{\cdot}265}. \qquad (19)$$

Note that the equilibrium values for Method 2 are less than those obtained from the frozen flow solutions, whereas the equilibrium results

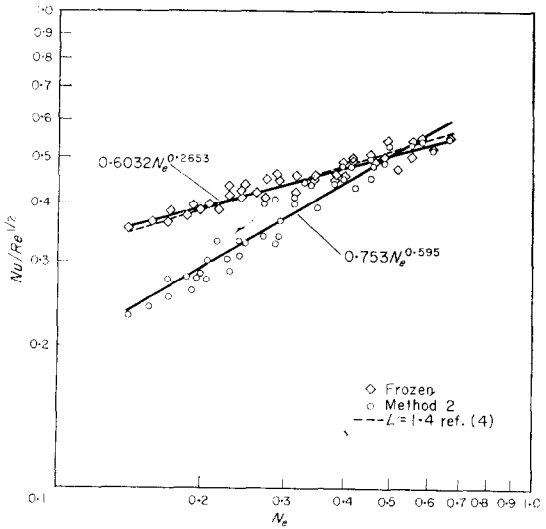

FIG. 6. Heat-transfer parameter, $Nu/(Re)^{1/2}$, vs. $\rho\mu$ ratio across a laminar boundary layer at a stagnation point.

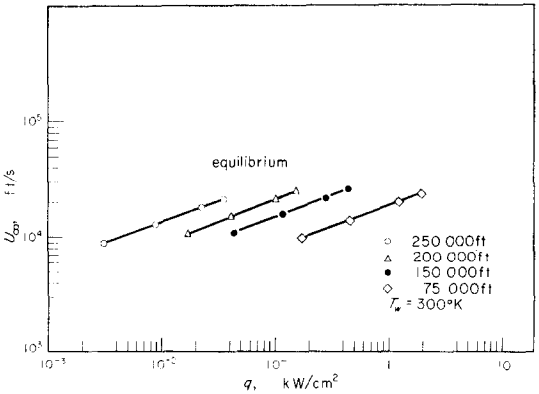

FIG. 7. Equilibrium stagnation point heat-transfer rates (R = 1 ft) vs. flight velocity.

for Method 1 yield values that are approximately equal to the frozen flow case. The actual heat-transfer rates to a body of 1-ft radius as determined from the above for equilibrium flow are shown in Fig. 7 as a function of flight velocity and altitude. The heating-rate equations obtained, using equations (18) and (19) are, respectively,

$$q_w = 0{\cdot}753\ Pr_w^{-1}\,(\rho_e\,\mu_e)^{0{\cdot}595}\,(\rho_w\,\mu_w)^{-0{\cdot}095}\,(du_e/dx)_s^{1/2}\,(h_e - h_w), \qquad (20)$$

$$q_w = 0{\cdot}603\ Pr_w^{-1}\,(\rho_e\,\mu_e)^{0{\cdot}265}\,(\rho_w\,\mu_w)^{0{\cdot}235}\,(du_e/dx)_s^{1/2}\,(h_e - h_w). \qquad (21)$$

B. Flat plate characteristics

Equations (7–9) with $\beta = 0$ and the appropriate boundary conditions yield the distributions of θ and z through a laminar boundary layer on a flat plate immersed in the uniform flow behind a normal shock traveling at the selected Mach numbers and altitudes.

Typical profiles of θ and c_a obtained by Method 2 are shown in Figs. 8 and 9 for the case $M_\infty = 24$, $T_w = 300°K$, altitude = 75 000 ft for both equilibrium and frozen flow. Fig. 10 shows the normalized chemical reaction energy and heat of formation distributions for this case. Trends shown here are the same as those obtained from the stagnation point solution.

The heat transfer parameter $Nu/(Re)^{1/2}$ is shown as a function of the $\rho\mu$ ratio in Fig. 11 for both equilibrium and frozen flow with $z(0) = 0$. Again, the results for all altitudes and Mach

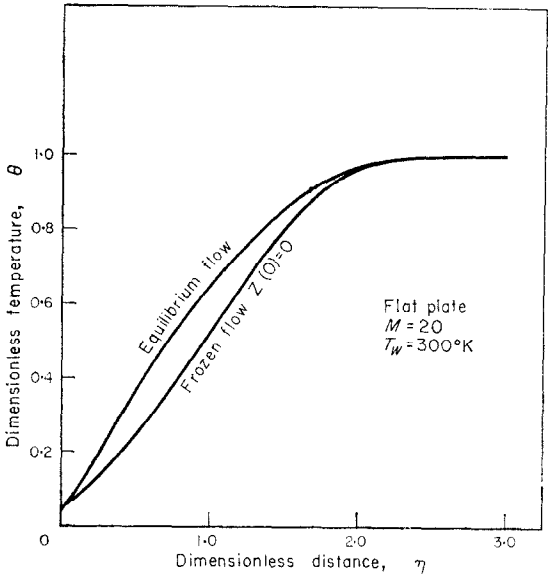

FIG. 8. Temperature distribution through a laminar flat plate boundary layer, Method 2, altitude = 75 000 ft.

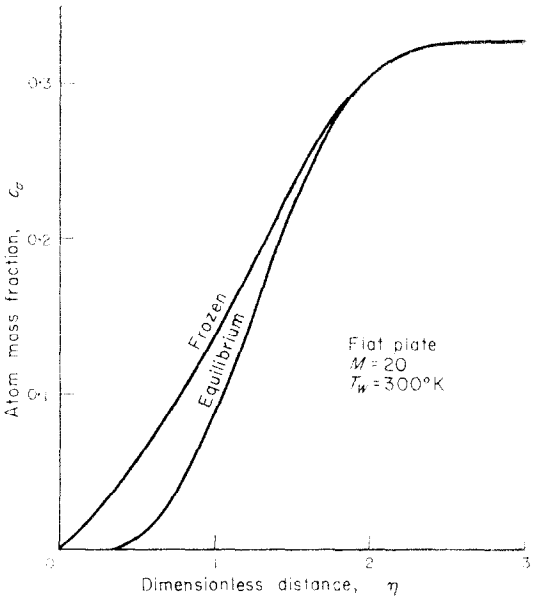

FIG. 9. Atom mass fraction distribution through a flat plate boundary layer, Method 2, altitude 75 000 ft.

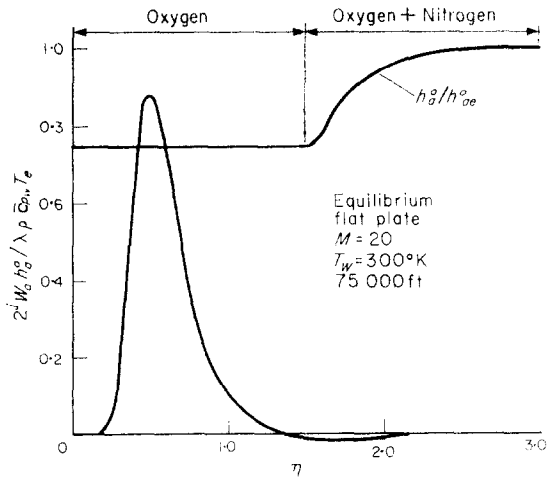

FIG. 10. Normalized chemical reaction energy and heat of dissociation distribution through a laminar flat plate boundary layer Method, 2.

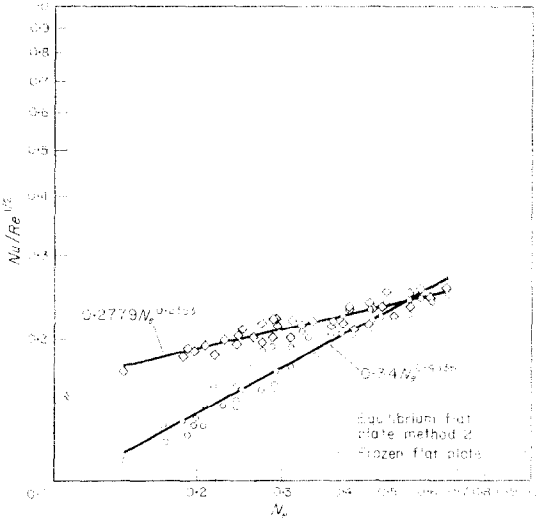

FIG. 11. Heat-transfer parameter, $Nu/(Re)^{1/2}$, vs. $\rho\mu$ ratio across a laminar flat plate boundary layer.

numbers considered were correlated by a least-squares fit given as

$$[Nu/(Re)^{1/2}]_w = 0{\cdot}34\, N_e^{0{\cdot}454} \tag{22}$$

for equilibrium flow and as

$$[Nu/(Re)^{1/2}]_w = 0{\cdot}28\, N_e^{0{\cdot}235} \tag{23}$$

for frozen flow with $z(0) = 0$. The above correlation yields the following heat-transfer rate equations:

$$q_w = 0{\cdot}34\, Pr_w^{-1}\, (\rho_e \mu_e)^{0{\cdot}454} (\rho_w \mu_w)^{0{\cdot}046}\, (u_e/x)^{1/2}\, (h_e - h_w) \tag{24}$$

$$q_w = 0{\cdot}28\, Pr_w^{-1}\, (\rho_e \mu_e)^{0{\cdot}235} (\rho_w \mu_w)^{0{\cdot}265}\, (u_e/x)^{1/2}\, (h_e - h_w) \tag{25}$$

for equilibrium and frozen flows with $z(0) = 0$. The heat-transfer rates at $x = 1$ ft for equilibrium flow are illustrated in Fig. 12 as a function of flight velocity and altitude. A summary curve of both the stagnation point and flat plate heat transfer is shown in Fig. 13.

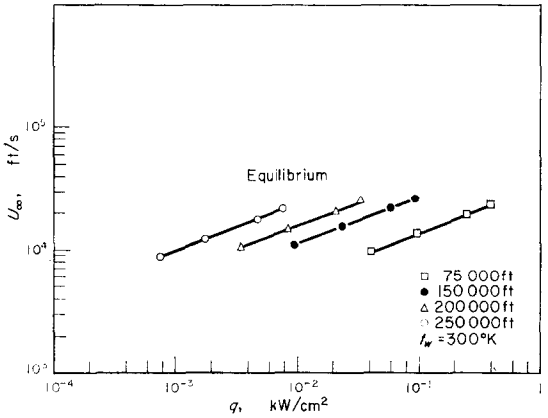

FIG. 12. Equilibrium flat plate heat-transfer rates ($x = 1$ ft) vs. flight velocity.

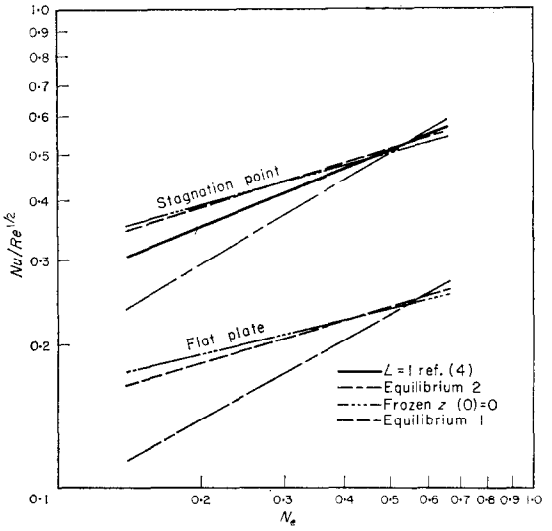

FIG. 13. Heat-transfer parameter, $Nu/(Re)^{1/2}$, vs. $\rho\mu$ ratio.

C. *Comparison of results with existing experimental data*

A number of heat-transfer measurements have been made at the stagnation point of models in shock tubes and tunnels simulating a portion of the range of flight conditions considered in this study [11, 12, 13]. The experimental studies were, in general, not carried out under the same velocity and pressure conditions, so that a direct comparison of experimental results is difficult. However, the experimental results available in the literature reveal a scatter of sufficient latitude to encompass the predictions of both Methods 1 and 2 at least through Mach numbers as high as 12 and altitudes up to 75 000 ft.

At low velocities (<13 000 ft/s) the data of [12] agree reasonably well with the Method 2 results, but at higher velocities (13 000–26 000 ft/s) the data of [11] clearly favor the results of Method 1.

6. CONCLUSIONS

The heat-transfer rates, considering variable Lewis number and variable heat of recombination at a stagnation point in equilibrium and frozen flows, may be given by

$$q_w = 0{\cdot}753\, Pr_w^{-1}\, (\rho_e \mu_e)^{0{\cdot}595} (\rho_w \mu_w)^{-0{\cdot}095}\, (du_e/dx)_s^{1/2}\, (h_e - h_w)$$

$$q_w = 0{\cdot}603\, Pr_w^{-1}\, (\rho_e \mu_e)^{0{\cdot}265} (\rho_w \mu_w)^{0{\cdot}235}\, (du_e/dx)_s^{1/2}\, (h_e - h_w)$$

whereas the flat plate heat-transfer rates for the two cases are

$$q_w = 0{\cdot}34\, Pr_w^{-1}\,(\rho_e \mu_e)^{0{\cdot}454}\,(\rho_w \mu_w)^{0{\cdot}046}\,(u_e/x)^{1{\cdot}2}\,(h_e - h_w)$$

$$q_w = 0{\cdot}28\, Pr_w^{-1}\,(\rho_e \mu_e)^{0{\cdot}235}\,(\rho_w \mu_w)^{0{\cdot}265}\,(u_e/x)^{1{\cdot}2}\,(h_e - h_w)$$

respectively. These results indicate that in the equilibrium case the external flow properties are the dominant influence determining heat transfer, as was found by previous investigators. In the case of completely frozen flow, however, the wall conditions are at least as important as the external flow conditions.

Using a variable heat of formation which allows for a distinction between oxygen and nitrogen recombination, gives results that are physically reasonable but somewhat lower than the equilibrium heat-transfer rates given by Fay and Riddell [4] and by Scala and Baulknight [5], but still within the experimental data scatter of [11], [12] and [13].

Hayes and Probstein [14] have summarized the effect of recombination of atoms on the heat transfer in a laminar boundary layer where the gas is a binary mixture of air atoms and molecules with Lewis number identically 1. Their primary conclusion is that it makes little difference upon heat transfer, whether the atoms recombine in the boundary layer or at the wall, which implies that all air atoms transfer equal amounts of recombination energy. However, air is more realistically a quaternary mixture and the oxygen and nitrogen atoms transport different amounts of recombination energy. The definition used here for a variable heat of formation in part accounts for this multiplicity of components in that almost all nitrogen atoms will recombine before oxygen recombination commences. Consequently, the equilibrium heat-transfer rates are lower than those of [4]. However, the frozen flow heat-transfer rates are essentially the same as those in [4], since atoms recombine only at the wall.

A particularly interesting consequence of the above definition of the heat of atom formation is the dominant effect of oxygen recombination occurring in the vicinity of the wall.

ACKNOWLEDGEMENTS

The authors should like to thank M. V. Morkovin for his valuable and encouraging comments and F. R. Riddell and N. Kemp for helpful criticism. Special thanks are due to C. Ellis for his considerable effort in programming this study for the IBM 7090.

REFERENCES

1. L. L. Moore, A solution of the laminar boundary layer equations for a compressible fluid with variable properties, including dissociation, *J. Aero/Space Sci.* **XIX**, 508 (1952).
2. F. F. Hansen, Note on the Prandtl number for dissociated air, *J. Aero/Space Sci.* **XX**, 789, 790 (1953).
3. M. F. Romig and F. J. Dore, Solutions of the compressible laminar boundary layer including the case of a dissociated free stream. Report ZA-7012, Convair-Astronautics, San Diego, California (1954).
4. J. A. Fay and F. R. Riddell, Theory of stagnation point heat transfer in dissociated air, *J. Aero/Space Sci.* **XXV**, 78–85 (1958).
5. S. M. Scala and C. W. Baulknight, Transport and thermodynamic properties in a hypersonic laminar boundary layer, *J. Amer. Rocket Soc.* **XXX** (4), 329 (1960).
6. R. E. Wilson, Real gas laminar boundary layer skin friction and heat transfer, *J. Aero/Space Sci.* **XXIX** (6), 640 (1962).
7. J. G. Logan and C. E. Treanor, Tables and thermodynamic properties of air from 3000°K. Report BE-1007-A3, Cornell Aeronautical Laboratory, Inc., Buffalo, New York (1957).
8. F. E. Hansen, Approximation for the thermodynamic and transport properties of high temperature air. *NACA* Report TN 4150 (1958).
9. R. Goulard, On catalytic recombination rates in hypersonic stagnation heat transfer, *Jet Propulsion*, **XXVIII** (11), 737 (1958).
10. S. J. Fenster and R. J. Heyman, Effect of variable heat of recombination on stagnation point heat transfer, *Readers Forum J. Aero/Space Sci.* **XXIX** (10), 1962.
11. P. H. Rose and W. I. Stark, Stagnation point heat transfer measurements in dissociated air, *J. Aeronaut. Sci.* **XXV** (2), 86 (1958).
12. B. D. Henshall, Stagnation point heat transfer rate measurements in the unexpanded flow ofthe N.P.L. hypersonic shock tunnel, N.P.L., C.P. 468 (1959).
13. A. B. Sabol, Measurements in a shock tube of heat transfer rates in the stagnation point of a 1·0-inch-diameter sphere for real-gas temperatures up to 7900°R. *NACA* Report TN 4354.
14. W. D. Hayes and R. F. Probstein, *Hypersonic Flow Theory*. Academic Press, New York (1959).

APPENDIX A

Method of machine solution

Evaluating equations (7–9) in terms of a binary mixture of air atoms and air molecules results in the following sets of equations:

Equilibrium Flow

$$(Nf'')' + ff'' + \beta\left[\frac{\rho_e}{\rho} - (f')^2\right] = 0$$

$$\frac{1}{Pr}(CN\theta')' + Cf\theta' + \frac{c_{ae}}{\bar{c}_{pw}}\frac{h_o^a}{T_e}\left[\frac{1}{Pr}(NLz')' + fz'\right] + \frac{N(\mu_e f'')^2}{\bar{c}_{pw}T_e} + \frac{NL\,c_{ae}}{Pr\,\bar{c}_{pw}}(c_{pa} - c_{pm})\theta' z' = 0$$

Frozen Flow

$$(Nf'')' + ff'' + \beta\left[\frac{\rho_e}{\rho} - (f')^2\right] = 0$$

$$\frac{1}{Pr}(CNz')' + fz' = 0$$

$$\frac{1}{Pr}(CN\theta')' + Cf\theta' + \frac{N(\mu_e f'')^2}{\bar{c}_{pw}T_e} + \frac{NL\,c_{ae}}{\bar{c}_{pw}\,Pr}(c_{pa} - c_{pm})\,\theta'\,z' = 0$$

where primes denote differentiation with respect to η.

Solution of the equations would have been very straightforward except for the fact that certain of the initial conditions were not known and had to be obtained as part of the solution. This was accomplished by an iterative procedure which will be described below.

Given the necessary tabular data and flight conditions, the solution began by assuming a set of values for the unknown initial conditions, $f''(0)$, $\theta'(0)$, and $Z'(0)$. If several cases were being computed consecutively, the guessed values were the values obtained in the previous solution. For the first case of any group, an arbitrary set of numbers was used which had been found to work satisfactorily in many cases. The equations were then integrated by means of Milne's method until a value of $f''(\eta)$ was obtained such that $f''(\eta) \leqslant \epsilon$.

This value for $f''(\eta)$ meant that $f'(\eta)$ was either approaching a horizontal asymptote or a maximum point. At this point integration was stopped, and the values of the functions compared with the required boundary conditions. If all conditions were met, it was assumed that the solution had been obtained. If any boundary condition was not satisfied, corrections were made to the initial conditions and a new iteration begun.

For the sake of simplicity, the method used to make corrections to the unknown initial conditions will be described only for the case of equilibrium flow. The extension to more than two functions is quite simple.

Corrections to $f''(0)$ and $\theta'(0)$ are obtained from the equations

$$\frac{\partial f'(\eta)}{\partial f''(0)}\Delta f''(0) + \frac{\partial f'(\eta)}{\partial \theta'(0)}\Delta\theta'(0) = 1 - f'(\eta)$$

$$\frac{\partial \theta(\eta)}{\partial f''(0)}\Delta f''(0) + \frac{\partial \theta(\eta)}{\partial \theta'(0)}\Delta\theta'(0) = 1 - \theta(\eta)$$

where $\Delta f''(0)$ and $\Delta\theta'(0)$ are the desired corrections and $f'(\eta)$ and $\theta'(\eta)$ are the values obtained using the previous approximations to the true values of the initial conditions. The partial derivatives were approximated by doing three initial iterations, the first one being the reference. For the second iteration $f''(0)$ was incremented by an amount $\delta f''(0)$ while $\theta'(0)$ remained fixed. Integration of the equations then resulted in new values for $f'(\eta)$ and $\theta(\eta)$ which differed from those of the first iteration by amounts $\delta' f(\eta)$ and $\delta\theta(\eta)$, respectively. Then,

$$\frac{\partial f'(\eta)}{\partial f''(0)} = \frac{\delta f'(\eta)}{\delta f''(0)}$$

and

$$\frac{\partial \theta(\eta)}{\partial f''(0)} = \frac{\delta\theta(\eta)}{\delta f''(0)}.$$

For the third iteration, $f''(0)$ was reset to its value at the first iteration and $\theta'(0)$ incremented by an amount $\delta\theta'(0)$. The partials with respect to $\theta'(0)$ were then computed in the same manner.

Validity of the solutions rests on the fact that all the boundary conditions are satisfied, and that decreasing the interval of integration does not change the results significantly. Uniqueness is indicated by the fact that different guesses at the unknown initial conditions always results in the same final solution.

APPENDIX B

Table 1. Method. 1. Equilibrium boundary layer

M	Alt.†	T_w	θ_w	N_e	c_{ae}	α	$f_{\eta\eta}(0)$	$\theta_\eta(0)$	$Nu/\sqrt{(Re)}$	β
10	75K	300°K	0·0928	0·4226	0·023	8·896	0·4778	0·4016	0·4288	0·5
14	150K	600°K	0·1184	0·3298	0·237	2·371	0·4543	0·6345	0·4417	0·5
20	200K	1000°K	0·1698	0·2896	0·4712	2·212	0·451	0·8781	0·4623	0·5
24	75K	300°K	0·03661	0·1701	0·495	2·227	0·3419	0·7105	0·3499	0·5
24	250K	300°K	0·0552	0·1971	0·507	2·245	0·3716	0·9837	0·3854	0·5
20	75K	300°K	0·042	0·2159	0·3275	2·360	0·2802	0·6042	0·1782	0
10	150K	1000°K	0·3065	0·5543	0·095	7·913	0·3936	0·4212	0·2437	0
24	250K	300°K	0·2757	0·1971	0·5069	2·245	0·2757	0·932	0·1826	0

Table 2. Method 2. Equilibrium boundary layer

M	Alt.	T_w	θ_w	N_e	c_{ae}	$c_a{}^*$	α	$f_{\eta\eta}(0)$	$\theta_\eta(0)$	$Nu/\sqrt{(Re)}$	β
10	75K	300°K	0·0928	0·4226	0·023	0·2346	8·896	0·4765	0·3955	0·4278	0·5
14	150K	600°K	0·1184	0·3298	0·237	0·2346	2·371	0·4519	0·5637	0·435	0·5
20	200K	1000°K	0·1698	0·2896	0·4712	0·2346	2·212	0·4481	0·6397	0·3368	0·5
24	75K	300°K	0·03661	0·1701	0·495	0·2346	2·227	0·3384	0·5480	0·2754	0·5
24	250K	300°K	0·0552	0·1971	0·507	0·2346	2·245	0·368	0·7049	0·2761	0·5
20	75K	300°K	0·042	0·2159	0·3275	0·2346	2·360	0·285	0·499	0·1471	0
10	150K	1000°K	0·3065	0·5543	0·095	0·2346	7·913	0·394	0·4151	0·2402	0
24	250K	300°K	0·2757	0·1971	0·5069	0·2346	2·245	0·2814	0·6775	0·1317	0
24	75K	300°K	0·03661	0·1701	0·495	0·200	2·245	0·3384	0·5474	0·2754	0·5
24	75K	300°K	0·03661	0·1701	0·495	0·170	2·245	0·3384	0·5474	0·2754	0·5
24	75K	300°K	0·03661	0·1701	0·495	0·150	2·245	0·3384	0·5478	0·2756	0·5

Table 3. Frozen boundary layer

M	Alt.	T_w	θ_w	N_e	c_{ae}	$f_{\eta\eta}(0)$	$\theta_\eta(0)$	$z_\eta(0)$	$z(0)$	$Nu/\sqrt{(Re)}$	β
10	250K	600°K	0·2469	0·5547	0·0433	0·5672	0·3229	0·3607	0	0·496	0·5
20	200K	300°K	0·0509	0·1987	0·4712	0·3425	0·3245	0·2519	0	0·3851	0·5
14	150K	1000°K	0·1973	0·3955	0·2370	0·4845	0·3026	0·3137	0	0·4533	0·5
24	75K	300°K	0·03661	0·1701	0·495	0·3181	0·3126	0·2405	0	0·3631	0·5
20	75K	300°K	0·042	0·2159	0·3275	0·2873	0·3167	0·2523	0	0·1868	0
10	250K	600°K	0·2469	0·5547	0·0433	0·3957	0·3067	0·338	0	0·2348	0
14	200K	1000°K	0·2217	0·417	0·2264	0·3686	0·2861	0·3016	0	0·2366	0
24	150K	300°K	0·0403	0·1416	0·7385	0·2607	0·3025	0·2186	0	0·1704	0

† The nomenclature 75 K, etc. designates 75 000 ft.

Résumé—On étudie l'échange thermique à travers une couche limite laminaire dissociée en utilisant une définition de la chaleur de dissociation variable permettant de faire une distinction entre l'oxygène et l'azote. Les résultats indiquent que la transmission de chaleur à travers une couche limite en équilibre est und peu moins grande que celle rapportée précédemment par d'autres auteurs. De plus, on trouve que, pour les conditions d'écoulement libre considérées, la recombinaison de l'oxygène (plutôt que celle de l'azote) est le phénomène prédominant dans la détermination de l'échange thermique à travers une couche limite en équilibre.

Zusammenfassung—Der Wärmeübergang durch eine dissoziierte laminaire Grenzschicht wurde untersucht unter Benützung veränderlicher Dissoziationswärmen, was eine Unterscheidung zwischen Sauerstoff und Stickstoff ermöglichte. Die Ergebnisse deuten darauf hin, dass der Wärmeübergang durch eine Gleichgewichtsgrenzschicht hier etwas unter dem kürzlich von anderen Forschern mitgeteilten liegt. Weiterhin wurde für den Bereich der betrachteten Freistromverhältnisse festgestellt, dass die Sauerstoffrekombination (eher als die des Stickstoffs) für die Bestimmung des Wärmeübergangs durch eine Gleichgewichtsgrenzschicht die dominierende Rolle spielt.

Аннотация—Исследуется теплообмен через диссоциированный ламинарный пограничный слой, используя понятие о переменной теплоте диссоциации, что позволяет проводить различие между кислородом и азотом. Результаты показывают, что теплообмен через равновесный пограничный слой несколько меньше, чем указывалось в ранее опубликованных работах других исследователей. Кроме того установлено, что в рассматриваемых условиях свободного течения рекомбинация кислорода (скорее, чем азота) является определяющим процессом при теплообмене через равновесный пограничный слой.